Scanning Laser Polarimetry with Enhanced Corneal Compensation and Optical Coherence Tomography in Normal and Glaucomatous Eyes

Mitra Sehi,[1] *Stephen Ume,*[1] *David S. Greenfield,*[1] *and Advanced Imaging in Glaucoma Study Group*[2]

Purpose. To examine the association between scanning laser polarimetry (SLP), using enhanced (ECC) and variable corneal compensation (VCC) with optical coherence tomography (OCT), and to compare their discriminating ability in the diagnosis of glaucoma.

Methods. Normal and glaucomatous eyes enrolled from four clinical sites underwent complete examination, automated perimetry, SLP-ECC, SLP-VCC, and OCT. Eyes were characterized in two groups based on the typical scan score (TSS): Normal birefringence pattern (NBP) was defined as a TSS of 80 to 100 and abnormal birefringence pattern (ABP) as TSS $\leq$ 79. For each of the six SLP parameters and five OCT parameters the areas under the receiver operating characteristic curve (AUROCs) were calculated to compare the discriminating ability of each imaging modality, to differentiate between normal and glaucomatous eyes.

Results. Ninety-five normal volunteers and 63 patients with glaucoma were enrolled. Average visual field mean deviation was -4.2 ± 4.3 dB in the glaucoma group. In eyes with NBP, SLP-ECC had significantly (all $P \leq 0.001$) greater correlation with OCT average, superior, and inferior retinal nerve fiber layer (RNFL; $r = 0.79, 0.67, 0.74$) compared with SLP-VCC ($r = 0.71, 0.43, 0.37$). In eyes with ABP, SLP-ECC had a significantly greater (all $P \leq 0.001$) correlation with OCT average, superior, and inferior RNFL ($r = 0.75, 0.73, 0.83$) compared with SLP-VCC ($r = 0.51, 0.22, 0.18$). The AUROC for OCT inferior average thickness (0.91) was similar ($P = 0.26$) to the TSNIT (temporal, superior, nasal, inferior, temporal) average obtained using SLP-ECC (0.87) and significantly ($P = 0.02$) greater than SLP-VCC (0.81).

Conclusions. Compared with SLP-VCC, SLP-ECC has significantly stronger correlations with OCT and may improve the discriminating ability for early glaucoma diagnosis. (*Invest Ophthalmol Vis Sci.* 2007;48:2099–2104) DOI:10.1167/iovs.06-1087

Scanning laser polarimetry (SLP) incorporates a confocal scanning laser ophthalmoscope with an integrated polarimeter that measures the amount of retardation of a polarized near-infrared laser beam as it passes through the RNFL.[1–6] The latest commercial polarimeter has an integrated variable corneal compensator (VCC) that determines and neutralizes the eye-specific corneal polarization axis and magnitude by using the concept of the macula as an intraocular polarimeter.[5,7–9] Studies have shown that SLP with VCC significantly improves the structure–function relationship,[10–13] agreement with other imaging technologies,[11,14] and discriminating power for the detection of glaucoma.[6,9,15,16]

It has been reported that in a subset of eyes, the SLP-VCC scans have atypical birefringence patterns (ABPs), so that the brightest areas of the retardation maps are not consistent with the histologically thickest portions of the peripapillary RNFL located along the superior and inferior arcuate bundles.[15]

An enhancement module (enhanced corneal compensation, ECC) has recently been described to eliminate artifacts associated with atypical birefringence patterns by removing the noise and enhancing the signal.[15–17] The ECC algorithm introduces a predetermined large birefringence bias to shift the measurement of the total retardation to a higher-value region, to remove noise and circumvent the problem of atypical patterns.[16]

The purpose of this investigation was to examine the association between scanning laser polarimetry using ECC and VCC with OCT measures and to compare their discriminating ability for glaucoma diagnosis.

Methods

Healthy volunteers and patients with glaucoma who met the eligibility criteria were prospectively enrolled at four clinical sites (Advanced Imaging in Glaucoma Study [AIGS] Group; refer to www.AIGStudy.net for full manual of procedures for the AIGS). All participants signed a consent form approved by the Institutional Review Board for Human Research of the participating institutions, which was in agreement with the provisions of the Declaration of Helsinki. All subjects underwent a complete ophthalmic examination, including slit lamp biomicroscopy, dilated stereoscopic examination, gonioscopy, Goldmann applanation tonometry, ultrasound pachymetry, and photography of the optic disc. Two reliable visual field (VF) examinations were obtained with standard automated perimetry (SAP; Humphrey Field Analyzer; Carl-Zeiss Meditec, Inc., Dublin, CA), by using the SITA (Swedish Interactive Threshold Algorithm) standard strategy program 24-2. Only one eye per subject was enrolled. If both eyes met eligibility criteria, one eye was selected randomly.

From the [1]Department of Ophthalmology, University of Miami Miller School of Medicine, Bascom Palmer Eye Institute, Palm Beach Gardens, Florida; [2]Glaucoma Study Group members are listed in the Appendix; entire study group staff is available at www.AIGStudy.net.

Presented in part at the annual meeting of the Association for Research in Vision and Ophthalmology, Fort Lauderdale, Florida, May 2006.

Supported in part by National Eye Institute Grants R01-EY013516 and R01-EY08684; the Maltz Family Endowment for Glaucoma Research, Cleveland, Ohio; a grant from Mr. Barney Donnelley, Palm Beach, FL; The Kessel Foundation, Bergenfield, New Jersey; and an unrestricted grant from Research to Prevent Blindness, New York, New York.

Submitted for publication September 12, 2006; revised November 2, 2006, and January 17, 2007; accepted March 20, 2007.

Disclosure: **M. Sehi**, None; **S. Ume**, None; **D. S. Greenfield**, Carl Zeiss Meditec, Heidelberg Engineering (C, R)

The publication costs of this article were defrayed in part by page charge payment. This article must therefore be marked "*advertisement*" in accordance with 18 U.S.C. §1734 solely to indicate this fact.

Corresponding author: Mitra Sehi, Bascom Palmer Eye Institute, University of Miami Miller School of Medicine, 7101 Fairway Drive, Palm Beach Gardens, FL 33418; msehi@med.miami.edu.

Inclusion criteria common to both groups consisted of refractive error between −7.00 and +3.00 D, best corrected visual acuity equal to or better than 20/40, age range between 40 and 79 years, reliable SAP (<33% rate of fixation losses, false positives, and false negatives), and no prior history of intraocular surgery except for uncomplicated cataract extraction. Any ocular disease other than glaucoma or cataract, visual acuity <20/40, peripapillary atrophy extending to 1.7 mm from the disc's center, retinal disease, or unreliable SAP caused the volunteer to be excluded from the study. Normal subjects consisted of volunteers such as office employees and friends or family members of patients with glaucoma. Normal subjects had no history of ocular disease except cataract, intraocular pressure (IOP) less than or equal to 21 mm Hg by Goldmann applanation tonometry, normal optic disc appearance based on clinical stereoscopic examination and review of stereodisc photography. All normal eyes had two SAP examinations with normal findings, defined as glaucoma hemifield test results within normal limits, and mean and pattern standard deviation (SD) of $P > 5\%$. Absence of glaucomatous optic neuropathy was defined as vertical cup-to-disc asymmetry <0.2, and intact neuroretinal rim without peripapillary hemorrhage, thinning, localized pallor, or RNFL defect. Glaucomatous optic neuropathy was defined as either cup-to-disc asymmetry between fellow eyes of greater than 0.2, rim thinning, notching, excavation, or RNFL defect. Patients with glaucoma had glaucomatous optic nerve damage and corresponding abnormal SAP defined as abnormal glaucoma hemifield test results and pattern SD outside 95% normal limits. Patients with SAP abnormalities had at least one confirmatory visual field examination.

SLP imaging (software version 5.5.0; Carl Zeiss Meditec, Inc.) was performed through undilated pupils. Three consecutive scans were obtained with VCC and ECC on the same day by the same examiner. The average of three measurements was used for the analysis. A primary scan was obtained before each measurement, to compensate for the corneal birefringence. Images that were obtained during eye movement were excluded, as well as unfocused, poorly centered images or images with a quality scan score of less than 8. A fixed concentric measurement band centered on the optic disc with a 3.2-mm outer and a 2.4-mm inner diameter was used to generate the peripapillary retardation measurements. SLP parameters used as outcome measures for this investigation included: TSNIT (temporal, superior, nasal, inferior, temporal) average, superior average, inferior average, nasal average, temporal average, TSNIT-SD, and the typical scan score (TSS). The nasal and temporal RNFL values were extracted by means of an electronic data export. OCT imaging (Stratus OCT, software ver. 4.0; Carl Zeiss Meditec, Inc.) was performed through undilated pupils using a fast RNFL thickness–acquisition protocol on the same day by the same examiner. The average of two measurements was used for the analysis. Images that were obtained during eye movement or were unfocused, were poorly centered, or had a signal strength of less than 7 were excluded. OCT parameters used as outcome measures for this investigation included average TSINT RNFL thicknesses.

Eyes were stratified into two groups based on the TSS obtained with SLP-VCC, as a measure of the level of atypia in the birefringence pattern. A normal birefringence pattern (NBP) was defined as a TSS of 80 or greater. An ABP was defined as a TSS of 79 or less,[15,18] based on previous work by Bagga et al.[15] in which the predictive probability of ABP was calculated using multiple logistic regression analysis; and eyes with a TSS below 80 had a greater prevalence of ABP images.

Statistical analysis was performed with commercial software (SPSS ver. 13.0; SPSS Inc., Chicago, IL). The independent-samples *t*-test, χ^2 test, and Mann-Whitney test were used to compare different measures between groups. Pearson correlation coefficients were calculated to investigate the association between OCT and SLP parameters and were compared by using a test of homogeneity with correlated data.[19] For each of the six SLP parameters and five OCT parameters, the areas under the receiver operator characteristic curve (AUROCs) were calculated, to compare the discriminating ability of each imaging modality to differentiate between normal and glaucomatous eyes. Significant differences in AUROC were determined by using the method of Hanley and McNeil.[20]

Results

Ninety-five normal volunteers and 63 patients with glaucoma were included in this investigation (mean ages, 54.6 ± 10.5 and 63.3 ± 9.0 years, respectively). Table 1 demonstrates the clinical characteristics of the study population. The visual field mean deviation and pattern SD were significantly different between the two groups ($P < 0.001$). No relationship was found between TSS and visual field mean deviation ($r = 0.08$; $P = 0.34$) or pattern SD ($r = 0.01$; $P = 0.89$). We evaluated the correlation between OCT and SLP parameters by using VCC and ECC in 116 patients with NBP and 42 patients with ABP. In eyes with NBP (Table 2), SLP-ECC had a significantly greater correlation with OCT than with SLP-VCC for the following parameters: TSNIT average ($r = 0.79$, ECC; $r = 0.71$, VCC; $P < 0.001$), superior ($r = 0.67$, ECC; $r = 0.43$, VCC; $P = 0.001$), and inferior ($r = 0.74$, ECC; $r = 0.37$, VCC; $P < 0.001$), but not temporal ($r = 0.15$, ECC; $r = 0.21$, VCC; $P = 0.59$) or nasal

Table 1. Clinical Characteristics of the Study Population*

	Normal ($n = 95$)	Glaucoma ($n = 63$)	*P*
Age (mean ± SD, y)	54.6 ± 10.5	63.3 ± 9.0	0.001†
Gender			0.18‡
Male	28	25	
Female	67	38	
Race			0.25‡
White non-Hispanic	86	51	
Black	6	5	
Asian	1	5	
Pacific Islander/Hawaiian	1	1	
Hispanic	1	1	
TSS with SLP-VCC (mean ± SD)	85.5 ± 18.1	79.3 ± 25.6	0.44§
TSS with SLP-ECC (mean ± SD)	98.9 ± 3.2	97.7 ± 8.1	0.72§
Visual field mean deviation (mean ± SD, dB)	−0.88 ± 2.4	−4.2 ± 4.3	<0.001§
Visual field pattern SD (mean ± SD, dB)	1.8 ± 1.5	5.4 ± 4.3	<0.001§

* $n = 158$.
† Independent-samples *t*-test.
‡ χ^2.
§ Mann-Whitney test.

TABLE 2. Correlation between OCT and Scanning Laser Polarimetry Parameters When Using VCC or ECC in Patients with NBP*

OCT Parameter	SLP Parameter	*r*	*P*	*P*†
Average RNFL	VCC-TSNIT average	0.71	<0.001	<0.001
	ECC-TSNIT average	0.79	<0.001	
Superior RNFL	VCC-superior	0.43	<0.001	0.001
	ECC-superior	0.67	<0.001	
Inferior RNFL	VCC-inferior	0.37	<0.001	<0.001
	ECC-inferior	0.74	<0.001	
Temporal RNFL	VCC-temporal	0.21	0.02	0.59
	ECC-temporal	0.15	0.12	
Nasal RNFL	VCC-nasal	0.65	<0.001	0.18
	ECC-nasal	0.59	<0.001	

* $n = 116$.
† Comparison of VCC and ECC correlation coefficients.

($r = 0.59$, ECC; $r = 0.65$, VCC; $P = 0.18$) RNFL thickness. In eyes with ABP (Table 3), SLP-ECC had a significantly ($P \leq 0.001$) greater correlation with OCT than with SLP-VCC for the following parameters: TSNIT average ($r = 0.75$, ECC; $r = 0.51$ VCC), superior ($r = 0.73$, ECC; $r = 0.22$ VCC), and inferior ($r = 0.83$, ECC; $r = 0.18$ VCC), but not temporal ($r = -0.10$, ECC; $r = 0.12$, VCC; $P = 0.19$) or nasal ($r = 0.53$, ECC; $r = 0.42$, VCC; $P = 0.22$) RNFL thicknesses.

Among the study population ($n = 158$), the TSS had an inverse correlation with measured RNFL in all sectors when SLP-VCC was used (TSNIT average, $r = -0.24$, $P = 0.002$; superior average, $r = -0.22$, $P = 0.006$; inferior average, $r = -0.28$, $P < 0.001$; temporal average, $r = -0.68$, $P < 0.001$; and nasal average, $r = -0.31$, $P = 0.03$). In normal volunteers, ECC had a significantly higher (all $P < 0.001$) correlation with OCT average, superior, and inferior ($r = 0.52$, $r = 0.33$, $r = 0.48$, respectively) RNFL thickness than with VCC ($r = 0.39$, $r = 0.006$, $r = 0.09$, respectively), but not for the temporal ($r = 0.002$, ECC; $r = 0.21$, VCC; $P = 0.09$) or nasal ($r = 0.54$, ECC; $r = 0.58$, VCC; $P = 0.45$) RNFL thicknesses. In patients with glaucoma, ECC had a significantly higher (all $P < 0.001$) correlation with OCT average, superior, and inferior RNFL thicknesses ($r = 0.66$, $r = 0.70$, $r = 0.69$, respectively) compared with VCC ($r = 0.45$, $r = 0.34$, $r = 0.24$, respectively), but not for the temporal ($r = 0.12$, ECC; $r = 0.02$, VCC; $P = 0.42$) or nasal ($r = 0.45$, ECC; $r = 0.38$, VCC; $P = 0.45$) RNFL thicknesses.

Table 4 illustrates the RNFL thicknesses measured by SLP-ECC, SLP-VCC, and OCT in normal volunteers and patients with glaucoma. The AUROCs and sensitivities at fixed specificities are provided for the study population ($n = 158$). The AUROC for SLP-ECC generated inferior thickness (0.85 ± 0.03) was significantly ($P = 0.0002$) greater than that for SLP-VCC (0.67 ± 0.05). There was no significant difference between the AUROC of SLP-ECC and SLP-VCC for superior ($P = 0.06$), temporal ($P = 0.42$), and nasal ($P = 0.74$) RNFL thicknesses. Figure 1 demonstrates AUROC curves for the best parameters obtained with SLP-VCC (TSNIT average), SLP-ECC (TSNIT average), and OCT (inferior average thickness). The AUROC for OCT inferior average thickness (0.91) was similar ($P = 0.26$) to the TSNIT average obtained with SLP-ECC (0.87) and was significantly ($P = 0.02$) greater than the TSNIT average obtained with SLP-VCC (0.81).

DISCUSSION

Glaucoma is a multifactorial optic neuropathy known to cause progressive loss of retinal ganglion cells and their axons, leading to accelerated reduction in the thickness of the RFNL. Imaging technologies such as SLP and OCT represent useful methods for objective detection and quantification of glaucomatous RNFL atrophy. Both technologies have been demonstrated to have high levels of reproducibility,[21–26] to incorporate age-matched normative data, and to allow noninvasive assessment of the peripapillary RNFL[27–31] through an undilated pupil.

SLP is a useful imaging technology for the diagnosis and monitoring of glaucoma. It is currently in its fifth commercial iteration, and considerable progress has been made in reducing artifacts originating from uncompensated anterior segment birefringence.[1,7–9,32] ABP images represent a challenge to SLP image interpretation by unfavorably altering the signal-to-noise ratio. ABP images have been reported to be more prevalent in older and myopic patients.[15] The mechanism remains obscure and is thought to be associated with reduced retinal pigment epithelial pigmentation and/or anomalous reflections from the posterior segment back to the detector. ECC represents a novel strategy for correction of ABP images by introducing a birefringence bias determined by using the birefringence pattern of the macular region, which is then mathematically removed point by point from the total birefringence pattern of the VCC image, to improve the signal and obtain a retardation pattern of the RNFL with reduced noise.[16] Toth and Hollo[16] reported a 10% to 15% prevalence of ABP images among 27 patients with glaucoma and 19 normal subjects and found that the ECC algorithm improved the mean TSS. Sehi et al.[18] reported that ECC parameters maintained a higher level of repeatability than does VCC.

In the present study, we hypothesized that by reducing the prevalence of ABP images, the ECC algorithm would improve the correlation between RNFL structural assessments obtained with SLP compared with OCT and thereby would improve the discriminating ability of SLP for glaucoma diagnosis. Our glaucoma cohort had an average visual field MD of −4.2 dB and consisted of patients with early damage, as judged using the Hodapp-Parrish-Anderson classification.[33] Indeed, we found that the correlations between structural measurements obtained using SLP-ECC and OCT were significantly greater than that of similar measurements obtained with the commercial SLP-VCC. Subgroup analysis demonstrated greater correlation coefficients between SLP-ECC and OCT in glaucomatous eyes than in normal eyes, and in eyes with ABP images than in those with NBP images. This finding is explained by the fact that SLP-VCC measures an artifactual increase in measured RNFL thickness in eyes with ABP, when using our data, and shows an inverse correlation between TSS (with lower values associated with increased ABP) and RNFL thickness parameters in all sectors. Glaucomatous eyes with ABP had an artifactual in-

TABLE 3. Correlation between OCT and Scanning Laser Polarimetry Parameters When Using VCC or ECC in Patients with ABP*

OCT Parameter	SLP Parameter	*r*	*P*	*P*†
Average RNFL	VCC-TSNIT average	0.51	0.001	0.001
	ECC-TSNIT average	0.75	<0.001	
Superior RNFL	VCC-superior	0.22	0.17	<0.001
	ECC-superior	0.73	<0.001	
Inferior RNFL	VCC-inferior	0.18	0.26	<0.001
	ECC-inferior	0.83	<0.001	
Temporal RNFL	VCC-temporal	0.12	0.45	0.19
	ECC-temporal	−0.10	0.54	
Nasal RNFL	VCC-nasal	0.42	0.005	0.22
	ECC-nasal	0.53	<0.001	

* $n = 42$.
† Comparison of VCC and ECC correlation coefficients.

TABLE 4. Values of Scanning Laser Polarimetry with ECC and VCC and OCT Parameters

Parameter	Glaucoma Mean (SD) (n = 63)	Normal Mean (SD) (n = 95)	P	AUROC Mean (SE)	Sensitivity at Specificity of 95% or Higher	Sensitivity at Specificity of 80% or Higher
ECC						
TSNIT average	44.5 (6.3)	54.0 (5.6)	<0.001	0.87 (0.03)	0.56	0.81
Superior average	55.2 (10.3)	67.8 (8.2)	<0.001	0.83 (0.04)	0.49	0.76
Inferior average	53.3 (10.0)	67.2 (8.8)	<0.001	0.85 (0.03)	0.54	0.67
Temporal average	18.0 (5.1)	16.7 (3.9)	0.17	0.45 (0.05)	0.24	0.25
Nasal average	30.4 (5.6)	34.8 (8.7)	0.001	0.65 (0.04)	0.32	0.38
TSNIT SD	21.0 (4.6)	27.4 (4.2)	<0.001	0.84 (0.3)	0.33	0.79
VCC						
TSNIT average	46.2 (8.0)	55.1 (6.2)	<0.001	0.81 (0.04)	0.54	0.67
Superior average	46.1 (11.6)	53.3 (7.6)	<0.001	0.73 (0.05)	0.48	0.57
Inferior average	43.5 (13.7)	47.6 (8.1)	0.03	0.67 (0.05)	0.41	0.56
Temporal average	32.3 (9.9)	30.6 (12.3)	0.35	0.41 (0.04)	0.03	0.06
Nasal average	36.8 (8.3)	43.2 (11.3)	<0.001	0.66 (0.04)	0.25	0.41
TSNIT SD	31.3 (12.6)	44.3 (13.8)	<0.001	0.80 (0.04)	0.14	0.73
OCT						
Average RNFL	74.8 (14.4)	99.3 (12.3)	<0.001	0.90 (0.03)	0.68	0.87
Superior RNFL	90.5 (23.0)	120.3 (19.6)	<0.001	0.84 (0.04)	0.38	0.76
Inferior RNFL	89.7 (22.0)	129.0 (18.7)	<0.001	0.91 (0.03)	0.67	0.87
Temporal RNFL	58.9 (16.2)	67.8 (11.9)	<0.001	0.66 (0.05)	0.41	0.44
Nasal RNFL	59.8 (15.1)	78.6 (17.7)	<0.001	0.79 (0.04)	0.57	0.62

AUROCs and sensitivities at fixed specificities are provided for the study population (n = 158).

crease in measured RNFL, causing the correlations between SLP-VCC and OCT-generated RNFL thickness parameters to be reduced. A manifest improvement was noted with the SLP-ECC algorithm. The overall prevalence of ABP in this population using SLP-VCC was small (27%). We speculate that compared with SLP-VCC, SLP-ECC would demonstrate a more robust correlation with other structure-based technologies in populations with a higher frequency and severity of ABP. We used a TSS cutoff of 80 in this study to define ABP based on previous work by Bagga et al.,[15] in which the predictive probability of ABP was calculated using multiple logistic regression analysis; eyes with a TSS less than 80 had a greater prevalence of ABP images. However, ABP images fall within a broad spectrum ranging from mild to severe, and a single cutoff may not always be appropriate.

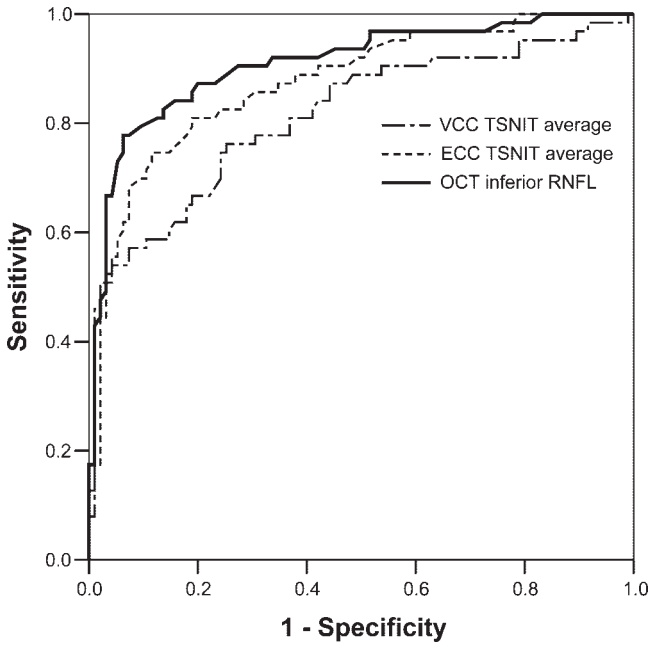

FIGURE 1. AUROCs for the best parameters obtained using scanning laser polarimetry with variable corneal compensation (TSNIT average, AUROC = 0.81), scanning laser polarimetry with enhanced corneal compensation (TSNIT average, AUROC = 0.87), and optical coherence tomography (inferior average thickness, AUROC = 0.91).

As demonstrated by Reus et al.,[34] ABP is predominantly seen in the nasal and temporal regions. In contrast, we did not find a significant improvement in correlation between SLP and OCT in the temporal and nasal thicknesses obtained using ECC compared with VCC. We speculate that this observation is based on the fact that 116 (73%) of 158 patients had images classified as NBP (TSS > 80). Recent data[35] suggest that ECC improves the discriminating power of SLP only in eyes with severe ABP (TSS < 60). In our study, only 23 (15%) of 158 eyes were classified as having a severe ABP. This study was therefore underpowered to provide a full evaluation of the impact of ECC in the nasal and temporal regions.

In our cohort of patients, the best parameters for discriminating between normal and glaucomatous eyes were the TSNIT average for SLP-ECC and SLP-VCC and the inferior average for OCT. It has been reported that the TSNIT average has the best discriminating ability when VCC is used.[36] We found the inferior RNFL thickness parameter of OCT to have the highest AUROC, similar to results in other studies.[37,38] Although both ECC and VCC correlated well with OCT, the ECC algorithm was superior to VCC, as the discriminating ability of ECC was not different from OCT, but the discriminating ability of VCC was significantly lower than OCT. The fact that ECC had a better correlation with OCT than did VCC suggests that SLP-ECC is a more robust measure for diagnosis of early glaucoma compared with the current commercial SLP-VCC. It is important to note that no single parameter or instrument should be used in isolation in clinical decisions regarding glaucoma diagnosis and that qualitative assessment of the optic nerve head is at least as sensitive and specific for glaucoma detection as quantitative methods of digital optic nerve head and nerve fiber layer imaging.[36,39] Furthermore, recent data[40] demonstrate that using combinations of parameters from selective structure- and function-based technologies can significantly improve the sensitivity and specificity of glaucoma detection compared with structure-based parameters in isolation.

We found that the diagnostic performance of SLP-ECC was significantly better than SLP-VCC. Although five of six of the SLP parameters had higher AUROC with ECC than with VCC, our study found a significant difference only in the inferior thickness parameter. It is important to point out that there are limitations to using the AUROC to assess the effectiveness of glaucoma diagnostic tests,[41] and recent data suggest that covariates such as optic disc size[42] and sophistication of analysis[41,43] should be taken into account when comparing the diagnostic performance of such tests. In addition, our AUROCs may be inflated to the extent that patients referred to a glaucoma practice who do not have glaucoma, could have imaging responses different from the normal control subjects used in this study.

In conclusion, SLP-ECC has significantly stronger correlations with OCT and may improve the diagnostic accuracy of early glaucoma compared with SLP-VCC. Further studies are needed to evaluate the ability of ECC to discriminate between normal and glaucomatous eyes compared with other structure- and function-based technologies.

APPENDIX

AIGS Group

David S. Greenfield (Principal Investigator), Carolyn D. Quinn, and Mitra Sehi, *University of Miami Miller School of Medicine*, *Bascom Palmer Eye Institute*, *Palm Beach Gardens*, *FL.*

David Huang, (Director), Rohit Varma (Principal Investigator), Vikas Chopra, Brian Francis, Don Minckler, and Ou Tan, *University of Southern California Keck School of Medicine*, *Doheny Eye Institute*, *Los Angeles*, *CA.*

Scott D. Smith (Principal Investigator) and Edward J. Rockwood, *Cleveland Clinic Foundation*, *Cole Eye Institute*, *Cleveland*, *OH.*

Joel S. Schuman (Principal Investigator), Robert Noecker, Zvia Eliash, Hiroshi Ishikawa, Gadi Wollstein, and Larry Kagemann, *University of Pittsburgh Medical Center*, *University of Pittsburgh School of Medicine*, *Pittsburgh*, *PA.*

References

1. Greenfield DS, Huang X-R, Knighton RW. Effect of corneal polarization axis on assessment of retinal nerve fiber layer thickness by scanning laser polarimetry. *Am J Ophthalmol*. 2000;129:715–722.
2. Dreher AW, Reiter K. Scanning laser polarimetry of the retinal nerve fiber layer. In: Goldstein DH, Chipman RA, eds. *Proc SPIE.* 1992;1746:34–41.
3. Dreher AW, Reiter KR. Retinal laser ellipsometry: a new method for measuring the retinal nerve fiber layer thickness distribution. *Clin Vision Sci*. 1992;7:481–488.
4. Weinreb RN, Dreher AW, Coleman A, Quigley H, Shaw B, Reiter K. Histopathologic validation of Fourier-ellipsometry measurements of retinal nerve fiber layer thickness. *Arch Ophthalmol*. 1990;108:557–560.
5. Knighton RW, Huang X-R, Greenfield DS. Analytical model of scanning laser polarimetry for retinal nerve fiber layer assessment. *Invest Ophthalmol Vis Sci*. 2002;43:383–392.
6. Choplin NT, Zhou Q, Knighton RW. Effect of individualized compensation for anterior segment birefringence on retinal nerve fiber layer assessments as determined by scanning laser polarimetry. *Ophthalmology*. 2003;110:719–725.
7. Garway-Heath DF, Greaney MJ, Caprioli J. Correction for the erroneous compensation of anterior segment birefringence with the scanning laser polarimeter for glaucoma diagnosis. *Invest Ophthalmol Vis Sci*. 2002;43:1465–1474.
8. Zhou Q, Weinreb RN. Individualized compensation of anterior segment birefringence during scanning laser polarimetry. *Invest Ophthalmol Vis Sci*. 2002;43:2221–2228.
9. Weinreb RN, Bowd C, Zangwill LM. Glaucoma detection using scanning laser polarimetry with variable corneal polarization compensation. *Arch Ophthalmol*. 2003;121:218–224.
10. Schlottman PG, De Cilla S, Greenfield DS, Caprioli J, Garway-Heath DF. Relationship between visual field sensitivity and retinal nerve fiber layer thickness as measured by scanning laser polarimetry. *Invest Ophthalmol Vis Sci*. 2004;45:1823–1829.
11. Bagga H, Greenfield DS, Feuer W, Knighton RW. Scanning laser polarimetry with variable corneal compensation and optical coherence tomography in normal and glaucomatous eyes. *Am J Ophthalmol*. 2003;135:521–529.
12. Bowd C, Zangwill LM, Weinreb RN. Association between scanning laser polarimetry measurements using variable corneal polarization compensation and visual field sensitivity in glaucomatous eyes. *Arch Ophthalmol*. 2003;121:961–966.
13. Reus NJ, Lemij HG. The relationship between standard automated perimetry and GDxVcCC measurements. *Invest Ophthalmol Vis Sci*. 2004;45:840–845.
14. Essock EA, Sinai MJ, Bowd C, Zangwill LM, Weinreb RN. Fourier analysis of optical coherence tomography and scanning laser polarimetry retinal nerve fiber layer measurements in the diagnosis of glaucoma. *Arch Ophthalmol*. 2003;121:1238–1245.
15. Bagga H, Greenfield DS, Feuer W. Quantitative assessment of atypical birefringence images using scanning laser polarimetry with variable corneal compensation. *Am J Ophthalmol*. 2005;139:437–446.
16. Toth M, Hollo G. Enhanced corneal compensation for scanning laser polarimetry on eyes with atypical polarisation pattern. *Br J Ophthalmol*. 2005;89:1139–1142.
17. Da Pozzo S, Marchesan R, Canziani T, Vattovani O, Ravalico G. Atypical pattern of retardation on GDx-VCC and its effect on retinal nerve fibre layer evaluation in glaucomatous eyes. *Eye*. 2006;20:769–775.
18. Sehi M, Guaqueta DC, Greenfield DS. An enhancement module to improve the atypical birefringence pattern using scanning laser polarimetry with variable corneal compensation. *Br J Ophthalmol*. 2006;90:749–753.
19. Meng XL, Rosenthal R, Rubin DB. Comparing correlated correlation coefficients. *Psych Bull*. 1992;111:172–175.
20. Hanley JA, McNeil BJ. A method of comparing the areas under receiver operating curves derived from the same cases. *Radiology*. 1983;148:839–843.
21. Schuman JS, Pedut-Kloizman T, Hertzmark E, et al. Reproducibility of nerve fiber layer thickness measurements using optical coherence tomography. *Ophthalmology*. 1996;103:1889–1898.
22. Blumenthal EZ, Williams JM, Weinreb RN, Girkin CA, Berry CC, Zangwill LM. Reproducibility of nerve fiber layer thickness measurements by use of optical coherence tomography. *Ophthalmology*. 2000;107:2278–2282.
23. Zangwill L, Berry CA, Garden VS, Weinreb RN. Reproducibility of retardation measurements with the nerve fiber analyzer II. *J Glaucoma*. 1997;6:384–389.
24. Villain MA, Greenfield DS. Peripapillary nerve fiber layer thickness measurement reproducibility using optical coherence tomography. *Ophthalmic Surg Lasers Imag*. 2003;34:33–37.
25. Rhee DJ, Greenfield DS, Chen PP, Schiffman J. Reproducibility of retinal nerve fiber layer thickness measurements using scanning laser polarimetry in pseudophakic eyes. *Ophthalmic Surg Lasers*. 2002;33:117–122.
26. Hoh ST, Greenfield DS, Liebmann JM, et al. Effect of pupillary dilation on retinal nerve fiber layer thickness measurement using scanning laser polarimetry. *J Glaucoma*. 1999;8:159–163.
27. Schuman JS, Hee MR, Puliafito CA, et al. Quantification of nerve fiber layer thickness in normal and glaucomatous eyes using optical coherence tomography. *Arch Ophthalmol*. 1995;113:586–596.
28. El Beltagi TA, Bowd C, Boden C, et al. Retinal nerve fiber layer thickness measured with optical coherence tomography is related to visual function in glaucomatous eyes. *Ophthalmology*. 2003;110:2185–2191.
29. Zangwill LM, Bowd C, Berry CC, et al. Discriminating between normal and glaucomatous eyes using the Heidelberg Retina Tomograph, GDx Nerve Fiber Analyzer, and Optical Coherence Tomograph. *Arch Ophthalmol*. 2001;119:985–993.

30. Zangwill LM, Williams J, Berry CC, Knauer S, Weinreb RN. A comparison of optical coherence tomography and retinal nerve fiber layer photography for detection of nerve fiber layer damage in glaucoma. *Ophthalmology*. 2000;107:1309–1315.
31. Nouri-Mahdavi K, Hoffman D, Tannenbaum D, Law SK, Caprioli J. Identifying early glaucoma with optical coherence tomography. *Am J Ophthalmol*. 2004;137:228–235.
32. Knighton RW, Huang XR. Analytical methods for scanning laser polarimetry. *Opt Express*. 2002;10:1179–1189.
33. Hodapp EP, Parrish RK, Anderson DR. *Clinical Decisions in Glaucoma.* St. Louis: Mosby; 1993;52–61.
34. Reus NJ, Zhou Q, Lemij HG. Enhanced imaging algorithm for scanning laser polarimetry with variable corneal compensation. *Invest Ophthalmol Vis Sci*. 2006;47:3870–3877.
35. Sehi M, Guaqueta DC, Feuer W, Greenfield DS. Scanning laser polarimetry with variable and enhanced corneal compensation in normal and glaucomatous eyes. *Am J Ophthalmol.* 2007;143:272–279.
36. Deleon-Ortega JE, Arthur SN, McGwin G Jr, Xie A, Monheit BE, Girkin CA. Discrimination between glaucomatous and nonglaucomatous eyes using quantitative imaging devices and subjective optic nerve head assessment. *Invest Ophthalmol Vis Sci*. 2006;47:3374–3380.
37. Medeiros FA, Zangwill LM, Bowd C, Weinreb RN. Comparison of the GDxVCC scanning laser polarimeter, HRT II confocal scanning laser ophthalmoscope, and Stratus OCT optical coherence tomograph for the detection of glaucoma. *Arch Ophthalmol*. 2004;122:827–837.
38. Kanamori A, Nagai-Kusuhara A, Escano MF, Maeda H, Nakamura M, Negi A. Comparison of confocal scanning laser ophthalmoscopy, scanning laser polarimetry and optical coherence tomography to discriminate ocular hypertension and glaucoma at an early stage. *Graefes Arch Clin Exp Ophthalmol*. 2006;244:58–68.
39. Greaney MJ, Hoffman DC, Garway-Heath DF, Nakla M, Coleman AL, Caprioli J. Comparison of optic nerve imaging methods to distinguish normal eyes from those with glaucoma. *Invest Ophthalmol Vis Sci*. 2002;43:140–145.
40. Shah NN, Bowd C, Medeiros FA, et al. Combining structural and functional testing for detection of glaucoma. *Ophthalmology*. 2006;113:1593–602.
41. Medeiros FA, Sample PA, Zangwill LM, Liebmann JM, Girkin CA, Weinreb RN. A statistical approach to the evaluation of covariate effects on the receiver operating characteristic curves of diagnostic tests in glaucoma. *Invest Ophthalmol Vis Sci*. 2006;47:2520–2527.
42. Medeiros FA, Zangwill LM, Bowd C, Sample PA, Weinreb RN. Influence of disease severity and optic disc size on the diagnostic performance of imaging instruments in glaucoma. *Invest Ophthalmol Vis Sci*. 2006;47:1008–1015.
43. Danesh-Meyer HV, Ku JY, Papchenko TL, Jayasundera T, Hsiang JC, Gamble GD. Regional correlation of structure and function in glaucoma, using the Disc Damage Likelihood Scale, Heidelberg Retina Tomograph, and visual fields. *Ophthalmology*. 2006;113:603–611.